Polynomial Chaos-Based Approach to Yield-Driven EM Optimization

Jianan Zhang, *Student Member, IEEE*, Chao Zhang, *Student Member, IEEE*, Feng Feng, *Member, IEEE*, Wei Zhang, *Student Member, IEEE*, Jianguo Ma, *Fellow, IEEE*, and Qi-Jun Zhang, *Fellow, IEEE*

***Abstract*— Yield-driven optimization is important in microwave design due to the uncertainties introduced in the manufacturing process. For the first time, we extend in this paper the use of polynomial chaos (PC) approach from electromagnetic (EM)-based yield estimation to EM-based yield optimization of microwave structures. We first formulate a novel objective function for yield-driven EM optimization. By incorporating the PC coefficients into the formulation, the objective function is analytically related to yield optimization variables, which are the nominal point. We then derive the sensitivity formulas of the PC coefficients with respect to the nominal point, following which we derive the sensitivities of the optimization objective function with respect to yield optimization variables. These sensitivities are then used in gradient-based optimization algorithms to find the optimal yield solution iteratively. The proposed objective function requires fewer EM simulations to provide reliable yield representation than that in the conventional Monte Carlo-based yield optimization approach. As a result, the number of EM simulations required to find the update direction and suitable step size for the change of the nominal point is reduced at each iteration of optimization. This allows the proposed approach to achieve similar yield increase using much fewer EM simulations or greater yield increase using similar number of EM simulations compared to the conventional yield optimization approach. The advantages of our proposed approach are demonstrated by yield-driven EM optimization of three waveguide filter examples.**

***Index Terms*— Electromagnetic (EM) optimization, EM sensitivities, microwave filters, polynomial chaos (PC), statistical analysis, yield estimation, yield optimization.**

I. Introduction

UNCERTAINTIES, introduced in the manufacturing process, pose inherent randomness on both geometrical dimensions and material properties of microwave components. Under this consideration, performing yield-driven optimization becomes an essential step in manufacturability-driven designs in a time-to-market development environment [1], [2]. The two decades after 1970 have witnessed the development of various yield optimization approaches, such as Monte Carlo-based approaches [1]–[5] and geometrical approaches [6]–[8]. These methods are developed mostly for circuit-based yield-driven design.

Since 1990s, electromagnetic (EM) simulations have been increasingly used in microwave design [9]–[14]. However, compared with the circuit-based yield-driven design, EM-based yield optimization is much more challenging. Simply replacing circuit simulations by EM simulations in conventional yield optimization approaches is not suitable because the requirement of a large number of EM simulations in yield optimization is computationally prohibitive. To alleviate this difficulty, space mapping optimization method has been introduced to the yield-driven design of microwave structures. Space mapping employs computationally fast coarse models to reduce the evaluation cost of the computationally expensive EM fine models. The number of EM simulations required in yield optimization is expected to be reduced as all the EM simulations are attributed to calibrating the coarse model at each space mapping iteration. In [15], space mapping neuromodels have been used in an efficient EM-based yield optimization procedure. In [16], space mapping has been combined with a modified ellipsoidal technique, and then, applied to yield optimization of microwave circuits. A response corrected tuning space mapping surrogate has been used for yield estimation and optimization in [17]. In [18], the generalized space mapping surrogate is reconstructed during yield optimization by parameter extraction. Jacobian matrixes of the EM responses are evaluated and used in the parameter extraction optimization process to enhance surrogate models. However, all the aforementioned space mapping-based approaches require the availability of an equivalent circuit coarse model. In many practical cases, equivalent circuit coarse models are not always available [19]. In this paper, we address the challenge of performing yield-driven EM optimization when explicit equivalent circuit coarse models are not available. More recently, feature-based methods have been studied and applied to yield estimation and optimization of microwave structures. In [20] and [21], a yield estimation technique exploiting feature-based statistical analysis has been presented. Yield optimization is then performed by optimizing the feature-based model using a pattern search algorithm. In [22], a correction method for feature parameters has been

Manuscript received November 24, 2017; revised February 27, 2018; accepted March 31, 2018. Date of publication May 22, 2018; date of current version July 2, 2018. This work was supported by the Natural Sciences and Engineering Research Council of Canada under Grant RGPIN-2017-06420. *(Corresponding author: Qi-Jun Zhang.)*

J. Zhang, W. Zhang, and Q.-J. Zhang are with the School of Microelectronics, Tianjin University, Tianjin, 300072, China, and also with the Department of Electronics, Carleton University, Ottawa, ON K1S 5B6, Canada (e-mail: jiananzhang@doe.carleton.ca; weizhang13@doe.carleton.ca; qjz@doe.carleton.ca).

C. Zhang and F. Feng are with the Department of Electronics, Carleton University, Ottawa, ON K1S 5B6, Canada (e-mail: chaozhang@doe.carleton.ca; fengfeng@doe.carleton.ca).

J. Ma is with the School of Computers, Guangdong University of Technology, Guangzhou 510006, China (e-mail: majg@tju.edu.cn).

Color versions of one or more of the figures in this paper are available online at http://ieeexplore.ieee.org.

Digital Object Identifier 10.1109/TMTT.2018.2834526

described to allow yield estimation of microwave filters. Yield optimization is then formulated as a constrained optimization problem and solved accordingly.

At each iteration of yield optimization, the prediction of yield values (also referred to as yield estimation) is typically involved. Recently, approaches based on polynomial chaos (PC) [23] have emerged as favorable alternatives for yield estimation and statistical analysis in the microwave area, such as those in [24]–[34]. In [24], for example, PC has been used to expand the time-domain electric and magnetic fields into orthogonal PC basis functions of uncertain mesh parameters. In [25], a decoupled PC and its applications to statistical analysis and yield estimation of high-speed interconnects have been reported. In [26], a nonintrusive formulation of the PC approach has been applied to quantify the uncertainties in deterministic models of the indoor radio channel. It has been demonstrated that the PC approach shows significant computational advantages over the traditional Monte Carlo analysis and can be regarded as a powerful tool in yield estimation and statistical analysis of microwave structures.

Compared to yield estimation, yield optimization has additional challenges. Unlike yield estimation where one fixed nominal point (usually regarded as the mean values of statistical parameters) is considered, in yield optimization, the nominal point is a variable that is updated iteratively, resulting in many nominal points to be considered. At each iteration of yield optimization, yield estimation needs to be performed with respect to one nominal point, and the update direction and suitable step size for the change of the nominal point need to be determined. These tasks have to be done repetitively from iteration to iteration during optimization, requiring a large number of EM simulations if we directly apply the conventional Monte Carlo-based or geometrical yield optimization approaches. Considering the computational advantages that PC offers in yield estimation, it is of great interest to explore the use of PC for yield optimization. However, how to use PC to facilitate the EM-based yield optimization of microwave structures still remains an open subject in the literature.

This paper proposes a novel PC-based approach to yield-driven EM optimization. For the first time, the use of PC approach is elevated from the EM-based yield estimation to EM-based yield optimization. The proposed approach provides systematic formulation and sensitivity formulas of EM-based yield optimization and does not require the availability of a coarse model. In the proposed approach, we first formulate a novel objective function for yield-driven EM optimization. By incorporating PC coefficients into the formulation, the objective function is analytically related to yield optimization variables, which are the nominal point. We then derive the sensitivity formulas of the PC coefficients with respect to the nominal point. The sensitivities of the objective function with respect to the nominal point are derived based on the sensitivity formulas of the PC coefficients. These sensitivities are then used in gradient-based optimization algorithms to find the optimal yield solution iteratively. The proposed objective function requires fewer EM simulations to provide reliable yield representation than that in the conventional Monte Carlo-based yield optimization approach. As a result, the number of EM simulations required to find the update direction and proper step size for the change of the nominal point is reduced at each iteration of optimization. This allows the proposed approach to achieve similar yield increase using much fewer EM simulations or greater yield increase using similar number of EM simulations compared to the conventional yield optimization approach. Three waveguide filter examples are used to demonstrate the advantages of our proposed approach.

This paper is organized as follows. In Section II, we briefly review the formulations of the PC approach and establish necessary notations for the descriptions of the proposed approach. In Section III, the proposed PC-based yield optimization approach is described in detail. Both the formulation and the sensitivity formulas of the proposed PC-based objective function for yield-driven EM optimization are presented. In Section IV, we demonstrate the advantages of the proposed approach using yield-driven EM optimization of three waveguide filter examples. In Section V, we conclude the paper.

II. Formulations of PC Approach

In this section, we give a brief overview of formulations of the PC approach and establish necessary notations for the descriptions of the proposed approach.

Let $\boldsymbol{x}$ represent the vector of n design parameters (e.g., geometrical parameters) of the EM structure, where $\boldsymbol{x} = [x_1, x_2, \ldots, x_n]^T$. Let $\boldsymbol{x}^0$ be the nominal point of $\boldsymbol{x}$. For statistical analysis of EM structures, the actual values of design parameters of the manufactured devices are spread around $\boldsymbol{x}^0$ following certain (uniform, normal, etc.) distributions. A key component of PC-based statistical analysis is performing a transformation of parameters from the original random parameters $\boldsymbol{x}$ to independent standard random parameters $\boldsymbol{\xi}$ and then applying the stochastic expansion in the transformed space (i.e., the "$\boldsymbol{\xi}$-space") [35]. Let $\boldsymbol{\xi} = [\xi_1, \ldots, \xi_n]^T$ be the vector of the independent standard random parameters. For example, $\xi_1, \ldots, \xi_n$ are with zero mean and unit variance if $x_1, x_2, \ldots, x_n$ have normal distributions, or with support $[-1, 1]$ if $x_1, x_2, \ldots, x_n$ are uniformly distributed. In the context of EM-based yield optimization, the change of $\boldsymbol{x}^0$ should be considered when performing the transformation as the nominal point is a variable. We thus denote this transformation as $\boldsymbol{\xi} = T(\boldsymbol{x}^0, \boldsymbol{x})$ with the reverse transformation denoted as

$$\boldsymbol{x} = T^{-1}(\boldsymbol{x}^0,\ \boldsymbol{\xi}). \tag{1}$$

The design goals are typically defined by a set of specifications imposed on the response of the EM structure at each frequency of interest. Let S_j be the jth design specification sample, where $j = 1, \ldots, m$. The symbol m denotes the number of specification samples, including samples for upper specifications and samples for lower specifications. Let m_u be the number of upper specification samples. For convenience of description, we assume that $S_1, \ldots, S_{m_u}$ are upper specification samples and that $S_{m_u+1}, \ldots, S_m$ are lower specification samples. Let $R_j(\boldsymbol{x})$ be the EM response at the frequency of interest that corresponds to S_j. As we focus on

yield optimization where the nominal point $\boldsymbol{x}^0$ is a variable, we intend to write $R_j(\boldsymbol{x})$ in a form where $\boldsymbol{x}^0$ is explicitly presented. Substituting the reverse transformation (1) into $R_j(\boldsymbol{x})$ allows us to have $R_j(\boldsymbol{x}) = R_j(T^{-1}(\boldsymbol{x}^0, \boldsymbol{\xi}))$. An error vector $\boldsymbol{e}(\boldsymbol{x})$ can be defined to measure the degree to which the response satisfies the design specifications as follows:

$$\boldsymbol{e}(\boldsymbol{x}) = \boldsymbol{e}(T^{-1}(\boldsymbol{x}^0, \boldsymbol{\xi})) = [e_1\ e_2 \cdots e_{m_u} \cdots e_m]^T \tag{2}$$

where the jth element in the error vector, $e_j(T^{-1}(\boldsymbol{x}^0, \boldsymbol{\xi}))$, is given as

$$e_j(T^{-1}(\boldsymbol{x}^0, \boldsymbol{\xi})) = \begin{cases} R_j(T^{-1}(\boldsymbol{x}^0, \boldsymbol{\xi})) - S_j, & \text{if } 1 \le j \le m_u \\ S_j - R_j(T^{-1}(\boldsymbol{x}^0, \boldsymbol{\xi})), & \text{if } m_u < j \le m. \end{cases} \tag{3}$$

In practice, it is possible to impose both an upper specification and a lower specification on the response at a common frequency of interest. For example, if S_{j_1} and S_{j_2} are the upper specification and the lower specification at a common frequency, respectively, then the responses $R_{j_1}(T^{-1}(\boldsymbol{x}^0, \boldsymbol{\xi}))$ and $R_{j_2}(T^{-1}(\boldsymbol{x}^0, \boldsymbol{\xi}))$ have the same values.

In PC-based statistical analysis of EM structures, the stochastic quantity of interest is $R_j(\boldsymbol{x})$. The functional form between $R_j(\boldsymbol{x})$ and $\boldsymbol{\xi}$ is approximated by the sum of weighted orthogonal basis polynomials in terms of the standard random parameters $\boldsymbol{\xi}$ as follows [23]:

$$R_j(\boldsymbol{x}) = R_j(T^{-1}(\boldsymbol{x}^0, \boldsymbol{\xi})) = \sum_{i=0}^{P} a_{ij}(\boldsymbol{x}^0)\Phi_i(\boldsymbol{\xi}) \tag{4}$$

where $\Phi_i(\cdot)$ is the generalized PC basis function. The optimal bases to construct the multivariate basis depend on the continuous probability distribution types of the design parameters. For example, Hermite polynomials are optimal for normal distribution while Legendre polynomials correspond to uniform distribution [35]. $a_{ij}(\boldsymbol{x}^0)$ is the weighting coefficient for the ith basis function Φ_i of the jth EM response $R_j(T^{-1}(\boldsymbol{x}^0, \boldsymbol{\xi}))$. $P+1$ is the number of terms in (4), given as [23]:

$$P + 1 = \frac{(n+D)!}{n! \cdot D!} \tag{5}$$

where n is the dimentionality of $\boldsymbol{x}$, and D is the highest polynomial order in the expansion.

In this paper, we focus on the nonintrusive stochastic collocation scheme (more specifically, the spectral projection approach) to compute the PC coefficients $a_{ij}(\boldsymbol{x}^0)$. Using the orthogonality condition of the PC basis functions $\Phi_i(\boldsymbol{\xi})$, the PC coefficients $a_{ij}(\boldsymbol{x}^0)$ can be found by projection [26]

$$a_{ij}(\boldsymbol{x}^0) = \frac{\int_{\Omega^n} R_j(T^{-1}(\boldsymbol{x}^0, \boldsymbol{\xi}))\Phi_i(\boldsymbol{\xi})\rho(\boldsymbol{\xi})d\boldsymbol{\xi}}{\int_{\Omega^n} \Phi_i^2(\boldsymbol{\xi})\rho(\boldsymbol{\xi})d\boldsymbol{\xi}} \tag{6}$$

where Ω^n is the n-dimensional space of all possible values of $\boldsymbol{\xi}$. $\rho(\boldsymbol{\xi})$ is the joint probability density function (PDF) of the standard random parameters $\boldsymbol{\xi}$. The definition of $\rho(\boldsymbol{\xi})$ is given as $\rho(\boldsymbol{\xi}) = \prod_{d=1}^{n} f(\xi_d)$, where $f(\xi_d)$ is the PDF of ξ_d, $d = 1, 2, \ldots, n$. Equation (6) is the same as that in [26] except that the change of the nominal point is considered. As $\boldsymbol{x}^0$ changes during yield optimization, the PC coefficients a_{ij} need to be reevaluated from iteration to iteration.

The multidimensional integration in (6) can be evaluated using numerical quadrature (see [26])

$$\int_{\Omega^n} R_j(T^{-1}(\boldsymbol{x}^0, \boldsymbol{\xi}))\Phi_i(\boldsymbol{\xi})\rho(\boldsymbol{\xi})d\boldsymbol{\xi} \approx \sum_{l=1}^{M} R_j(T^{-1}(\boldsymbol{x}^0, \boldsymbol{\xi}^{(l)}))\Phi_i(\boldsymbol{\xi}^{(l)})w^{(l)} \tag{7}$$

$$\int_{\Omega^n} \Phi_i^2(\boldsymbol{\xi})\rho(\boldsymbol{\xi})d\boldsymbol{\xi} \approx \sum_{l=1}^{M} \Phi_i^2(\boldsymbol{\xi}^{(l)})w^{(l)} \tag{8}$$

where $\boldsymbol{\xi}^{(l)}$ and $w^{(l)}$ are the integration quadrature points (also called "nodes") and weights in the "$\boldsymbol{\xi}$-space," respectively. M is the total number of integration quadrature points. $R_j(T^{-1}(\boldsymbol{x}^0, \boldsymbol{\xi}^{(l)}))$ is the EM response evaluated at the lth sampling point in the original random space. As an example, assuming that the design parameters are independently Gaussian distributed with mean values $x_1^0, x_2^0, \ldots, x_n^0$ and standard deviations $\sigma_1, \sigma_2, \ldots, \sigma_n$, the lth sample in the original space is given as

$$T^{-1}(\boldsymbol{x}^0, \boldsymbol{\xi}^{(l)}) = \boldsymbol{x}^0 + \Gamma\boldsymbol{\xi}^{(l)} \tag{9}$$

where Γ is a diagonal matrix containing the standard deviations for all the design parameters, i.e., $\Gamma = \text{diag}\{\sigma_1\ \sigma_2\ \cdots\ \sigma_n\}$. To reduce the computational costs for multidimensional numerical integration in (7) and (8), sparse grid techniques based on the Smolyak algorithm are typically applied [36]. In many cases, this can accurately approximate multidimensional integrals with substantially fewer quadrature points.

As the change of $\boldsymbol{x}^0$ does not affect the numerical quadrature in (8), for notational convenience, we define b_i as follows:

$$b_i = \sum_{l=1}^{M} \Phi_i^2(\boldsymbol{\xi}^{(l)})w^{(l)}. \tag{10}$$

b_i is problem independent. It only depends on M and the distribution types of standard random parameters $\boldsymbol{\xi}$. Therefore, b_i can be determined before one performs yield optimization. Based on (6)–(8) and (10), the PC coefficients can be computed from

$$a_{ij}(\boldsymbol{x}^0) = \frac{1}{b_i}\sum_{l=1}^{M} R_j(T^{-1}(\boldsymbol{x}^0, \boldsymbol{\xi}^{(l)}))\Phi_i(\boldsymbol{\xi}^{(l)})w^{(l)} \tag{11}$$

where $\Phi_i(\boldsymbol{\xi}^{(l)})$ and $w^{(l)}$ are the constants for yield optimization.

One valuable feature of the PC approach is that once the coefficients $a_{ij}(\boldsymbol{x}^0)$ are computed, the statistical properties of the stochastic quantity $R_j(T^{-1}(\boldsymbol{x}^0, \boldsymbol{\xi}))$, e.g., mean $\mu_j(\boldsymbol{x}^0)$ and variance $\sigma_j^2(\boldsymbol{x}^0)$ can be obtained analytically through these coefficients in a simple closed form [26]

$$\mu_j(\boldsymbol{x}^0) = E(R_j) = a_{0j}(\boldsymbol{x}^0) \tag{12}$$

$$\sigma_j^2(\boldsymbol{x}^0) = E[(R_j - \mu_j)^2] = \sum_{i=1}^{P} a_{ij}^2(\boldsymbol{x}^0)b_i. \tag{13}$$

III. Proposed PC-Based Yield Optimization Approach

In this section, our proposed PC-based yield optimization approach is presented in detail. In Section III-A, we incorporate the PC coefficients into the objective function for yield-driven EM optimization. By taking full advantage of the statistical properties provided by the PC coefficients, the number of EM simulations required to achieve reliable yield representation is reduced. In Section III-B, we derive the sensitivity formulas of the PC coefficients with respect to the nominal point, followed by the derivation of the sensitivities for the proposed objective function. These sensitivities are then used in the gradient-based optimization algorithms to find the optimal yield solution iteratively. Finally, the proposed yield optimization process is summarized into a stepwise algorithm.

A. Formulation of the Objective Function for Yield-Driven EM Optimization Incorporating PC Coefficients

Bandler and Chen [1] presented a one-sided least pth objective function $U(\boldsymbol{x}^0)$ that was well suited to accelerating yield optimization. The objective function $U(\boldsymbol{x}^0)$ is congregated from the simulated responses related to design specifications for all the circuit outcomes randomly generated around the nominal point. Increase of the yield can be achieved by minimizing $U(\boldsymbol{x}^0)$ since such minimization leads to a better center in the feasible region [2]. In this paper, we use the formulation in [1] as a starting point and propose a new and different objective function to facilitate yield-driven EM optimization.

In the statistical approach to microwave design, we consider that the random outcomes of the design parameters $\boldsymbol{x}$ are actually spread around the nominal point $\boldsymbol{x}^0$ following their statistical distributions and tolerances [15]. The kth random outcome of $\boldsymbol{x}$ can be denoted as

$$\boldsymbol{x}^k = T^{-1}(\boldsymbol{x}^0, \boldsymbol{\xi}^k), \quad k = 1, \ldots, N \tag{14}$$

where N is the total number random outcomes of $\boldsymbol{x}$. $\boldsymbol{\xi}^k$ is the vector of standard random parameters, which corresponds to $\boldsymbol{x}^k$. In this paper, to distinguish the random outcomes of $\boldsymbol{x}$ in the Monte Carlo analysis from the sparse grid samples of $\boldsymbol{x}$ in the PC approach, we use k $(k = 1, \ldots, N)$ to represent the index of random outcomes and use l $(l = 1, \ldots, M)$ to represent the index of sparse grid samples.

Suppose that $H_p(\cdot)$ represents the one-sided least pth function. Following [1], the objective function $U(\boldsymbol{x}^0)$ for the Monte Carlo-based yield optimization is given as [1]

$$U(\boldsymbol{x}^0) = H_p(\boldsymbol{u}(\boldsymbol{x}^0)) \tag{15}$$

where $\boldsymbol{u} = [u_1, u_2, \ldots, u_N]^T$. The kth component in $\boldsymbol{u}$ is defined as

$$u_k = \alpha_k H_q(\boldsymbol{e}(T^{-1}(\boldsymbol{x}^0, \boldsymbol{\xi}^k))), \quad k = 1, \ldots, N \tag{16}$$

where q is an index indicating the norm used for $\boldsymbol{e}$ while p is an index indicating the norm used for $\boldsymbol{u}$. The specific definition of the least pth norms $(p = 1, 2, \ldots, \infty)$ can be found in [1]. If we use $p = 1$ and $q = 1$ (as used in [1]) and take the weighting factor $\alpha_k = 1$, the objective function $U(\boldsymbol{x}^0)$ will take the following form [1]:

$$U(\boldsymbol{x}^0) = \sum_{k \in K} \sum_{j \in J(\boldsymbol{x}^k)} e_j(T^{-1}(\boldsymbol{x}^0, \boldsymbol{\xi}^k)) \tag{17}$$

$$J(\boldsymbol{x}^k) = \{j | e_j(T^{-1}(\boldsymbol{x}^0, \boldsymbol{\xi}^k)) > 0\} \tag{18}$$

$$K = \{k | J(\boldsymbol{x}^k) \neq \emptyset\}. \tag{19}$$

The objective function defined in (17) typically requires the number of outcomes N to be reasonably sufficient to make the minimization of (17) effective. It works efficiently if the computation of responses is by circuit simulations. However, it is not computationally efficient to directly apply (17) to yield-driven EM optimization. The reason is that in each iteration of yield optimization, the EM simulations need to be done N times, where N is the number of random outcomes of $\boldsymbol{x}$. Furthermore, those simulations have to be redone from iteration to iteration as the nominal point $\boldsymbol{x}^0$ is changed, resulting in a large number of EM simulations.

To alleviate this difficulty, we propose a new formulation of the objective function inspired by the fact that the statistical properties of the EM response can be obtained analytically through the PC coefficients. Provided that the computation of the PC coefficients is accurate and not too expensive, we can take full advantage of the statistical properties offered by PC such that the number of EM simulations required to achieve reliable yield representation is reduced. In terms of nonintrusive PC approaches, it has been shown that the number of integration samples M required to obtain accurate PC coefficients is much fewer than the number of outcomes N required in the Monte Carlo analysis [26]. Thus, if we can use the PC coefficients properly to formulate a new objective function, the computational costs to achieve reliable yield representation can be reduced and the overall yield optimization process can be expedited. In the subsequent descriptions, we follow this idea to propose our PC-based yield optimization approach.

As shown in (4), for each specification sample S_j, we have one response $R_j(T^{-1}(\boldsymbol{x}^0, \boldsymbol{\xi}))$ and one corresponding set of PC coefficients a_{ij}, $i = 0, 1, \ldots, P$. In order to incorporate the PC coefficients into EM-based yield optimization, we need to reorganize the objective function defined in (17) into a form where the error element $e_j(T^{-1}(\boldsymbol{x}^0, \boldsymbol{\xi}^k))$ is accumulated first with respect to each specification sample S_j then with respect to each set of design parameters of the outcomes $\boldsymbol{x}^k$. By doing this, the statistical properties of the responses computed from the PC coefficients can be exploited. To achieve this, we rewrite the original objective function $U(\boldsymbol{x}^0)$ in (17) by swapping the order of the summations, and at the same time rearrange the elements in J and K as follows:

$$U(\boldsymbol{x}^0) = \sum_{j \in \bar{J}} \sum_{k \in \bar{K}_j} e_j(T^{-1}(\boldsymbol{x}^0, \boldsymbol{\xi}^k)) \tag{20}$$

$$\bar{K}_j = \{k | e_j(T^{-1}(\boldsymbol{x}^0, \boldsymbol{\xi}^k)) > 0\} \tag{21}$$

$$\bar{J} = \{j | \bar{K}_j \neq \emptyset\} \tag{22}$$

where $\bar{K}_j$ is a set containing all the indices of the outcomes whose responses violate the specification sample S_j. $\bar{J}$ is a set

containing all the indices of the specification samples that are violated by at least one outcome.

As shown in (3), the error element $e_j(T^{-1}(\boldsymbol{x}^0, \boldsymbol{\xi}^k))$ is calculated differently for upper and lower specifications. For convenience of description, we divide the reorganized objective function (20) into two parts according to the design specification type of S_j as follows:

$$U(\boldsymbol{x}^0) = \sum_{j\in\bar{J}_u}\sum_{k\in\bar{K}_j} e_j(T^{-1}(\boldsymbol{x}^0, \boldsymbol{\xi}^k)) + \sum_{j\in\bar{J}_l}\sum_{k\in\bar{K}_j} e_j(T^{-1}(\boldsymbol{x}^0, \boldsymbol{\xi}^k)) \tag{23}$$

where $\bar{J}_u$ and $\bar{J}_l$ contain the indices of the upper and lower specification samples that are violated by at least one outcome, respectively, that is,

$$\bar{J}_u = \{j | j \in \bar{J}, 1 \le j \le m_u\} \tag{24}$$

$$\bar{J}_l = \{j | j \in \bar{J}, m_u < j \le m\}. \tag{25}$$

It can be noted that $\bar{J}_u \cup \bar{J}_l = \bar{J}$.

Let N_j^{fail} be the number of elements in $\bar{K}_j$. N_j^{fail} represents the number of outcomes whose responses fail to satisfy the specification S_j. If the total number of outcomes N goes to infinity, then the statistical properties of $\sum_{k\in\bar{K}_j} e_j(T^{-1}(\boldsymbol{x}^0, \boldsymbol{\xi}^k))$ can be represented more accurately by an integral form as follows:

$$\begin{aligned}
&\lim_{N\to\infty}\frac{1}{N}\sum_{k\in\bar{K}_j} e_j(T^{-1}(\boldsymbol{x}^0, \boldsymbol{\xi}^k)) \\
&= \frac{1}{N}E(e_j(T^{-1}(\boldsymbol{x}^0, \boldsymbol{\xi}))\cdot N_j^{\text{fail}} \\
&= E[(R_j - S_j) \mid R_j > S_j]\cdot\frac{N_j^{\text{fail}}}{N} \\
&= \frac{\int_{S_j}^{\infty}(R_j - S_j)f(R_j)dR_j}{\int_{S_j}^{\infty} f(R_j)dR_j}\cdot\frac{N_j^{\text{fail}}}{N} \\
&= \frac{\int_{S_j}^{\infty}(R_j - S_j)f(R_j)dR_j}{N_j^{\text{fail}}/N}\cdot\frac{N_j^{\text{fail}}}{N} \\
&= \int_{S_j}^{\infty}(R_j - S_j)f(R_j)dR_j \\
&= -S_j\int_{S_j}^{\infty} f(R_j)dR_j + \int_{S_j}^{\infty} R_j f(R_j)dR_j
\end{aligned} \tag{26}$$

where $j \in \bar{J}_u$, $R_j = R_j(T^{-1}(\boldsymbol{x}^0, \boldsymbol{\xi}))$, which can be expressed as truncated series expansion as shown in (4) if we apply the PC approach. $E[(R_j - S_j) \mid R_j > S_j]$ represents the mean value of $(R_j - S_j)$ conditional on $R_j > S_j$. $f(R_j)$ denotes the PDF of R_j.

Similarly, the statistical properties of $\sum_{k\in\bar{K}_j} e_j(T^{-1}(\boldsymbol{x}^0, \boldsymbol{\xi}^k))$, $j \in \bar{J}_l$, can be represented more accurately by an integral form as follows:

$$\begin{aligned}
&\lim_{N\to\infty}\frac{1}{N}\sum_{k\in\bar{K}_j} e_j(T^{-1}(\boldsymbol{x}^0, \boldsymbol{\xi}^k)) \\
&= S_j\int_{-\infty}^{S_j} f(R_j)dR_j - \int_{-\infty}^{S_j} R_j f(R_j)dR_j.
\end{aligned} \tag{27}$$

It is noted that (26) and (27) have different intervals for the integration, i.e., (26) has interval $[S_j, \infty)$ while (27) has interval $(-\infty, S_j]$.

For notational convenience, we define $\bar{u}_j(\boldsymbol{x}^0)$ as a yield indicator with respect to the specification sample S_j as follows:

$$\bar{u}_j(\boldsymbol{x}^0) = \begin{cases} -S_j\displaystyle\int_{S_j}^{\infty} f(R_j)dR_j + \int_{S_j}^{\infty} R_j f(R_j)dR_j, & j \in \bar{J}_u \\ S_j\displaystyle\int_{-\infty}^{S_j} f(R_j)dR_j - \int_{-\infty}^{S_j} R_j f(R_j)dR_j, & j \in \bar{J}_l. \end{cases} \tag{28}$$

$\bar{u}_j(\boldsymbol{x}^0)$ can be regarded as an indicator of the yield because a small value of $\bar{u}_j(\boldsymbol{x}^0)$ basically represents that there are few outcomes whose responses violate the specification sample S_j, indicating a high yield. Therefore, reducing $\bar{u}_j(\boldsymbol{x}^0)$ is expected to lead to an increase of the yield.

Given μ_j, σ_j^2, and higher moments of R_j [35], $f(R_j)$ in (28) can be approximated using the existing PDF estimation techniques, e.g., the moment matching technique [37] and the maximum entropy technique [38]. Then, the integrals in $\bar{u}_j(\boldsymbol{x}^0)$ can be evaluated by applying the Gauss quadratures developed in [39]. In this paper, to analytically relate $\bar{u}_j(\boldsymbol{x}^0)$ to the nominal point through the PC coefficients, we consider a special case where the EM response R_j follows normal distribution with μ_j and σ_j as its mean and standard deviation, respectively. In the following descriptions, we show how $\bar{u}_j(\boldsymbol{x}^0)$ is analytically related to the nominal point through PC coefficients under such consideration.

Based on (12) and (13), the first term of $\bar{u}_j(\boldsymbol{x}^0)$, $j \in \bar{J}_u$, can be related to the nominal point $\boldsymbol{x}^0$ through PC coefficients as follows:

$$-S_j\int_{S_j}^{\infty} f(R_j)dR_j = S_j\left(\phi\left(\frac{S_j - a_{0j}(\boldsymbol{x}^0)}{\sqrt{\sum_{i=1}^{P} a_{ij}^2(\boldsymbol{x}^0)b_i}}\right) - 1\right) \tag{29}$$

where $\phi(\cdot)$ is the cumulative distribution function of the standard normal distribution. a_{0j} and a_{ij} are the PC coefficients as functions of yield optimization variables $\boldsymbol{x}^0$.

For notational convenience, let $\gamma_j(\boldsymbol{x}^0)$ be defined as

$$\gamma_j(\boldsymbol{x}^0) = \frac{S_j - a_{0j}(\boldsymbol{x}^0)}{\sqrt{\sum_{i=1}^{P} a_{ij}^2(\boldsymbol{x}^0)b_i}}, \qquad j \in \bar{J}_u \cup \bar{J}_l. \tag{30}$$

$\phi(\gamma_j(\boldsymbol{x}^0))$ represents the probability that R_j satisfies the specification S_j in case $j \in \bar{J}_u$ or violates S_j in case $j \in \bar{J}_l$.

To analytically relate the second term of $\bar{u}_j(\boldsymbol{x}^0)$, $j \in \bar{J}_u$, to the nominal point through PC coefficients, we are interested in finding the mean value of the EM response R_j under the condition that R_j violates the upper specification S_j. Let $E(R_j \mid R_j > S_j)$ be the mean value of R_j conditional on $R_j > S_j$. Then, $\int_{S_j}^{\infty} R_j f(R_j)dR_j$ can be analytically related

to the nominal point $\boldsymbol{x}^0$ as follows [40]:

$$\begin{aligned}\int_{S_j}^{\infty} R_j f(R_j) dR_j &= E(R_j \mid R_j > S_j) \cdot \int_{S_j}^{\infty} f(R_j) dR_j \\ &= \mu_j (1 - \phi(\gamma_j(\boldsymbol{x}^0))) + \frac{1}{\sqrt{2\pi}} \sigma_j \cdot e^{-\frac{1}{2}\gamma_j^2(\boldsymbol{x}^0)} \end{aligned} \tag{31}$$

where μ_j and σ_j can be computed from PC coefficients as given by (12) and (13).

The PC coefficients are incorporated into $\bar{u}_j(\boldsymbol{x}^0)$ for the upper specifications by substituting (12)–(13) and (29)–(31) into $\bar{u}_j(\boldsymbol{x}^0)$, $j \in \bar{J}_u$, as follows:

$$\bar{u}_j(\boldsymbol{x}^0) = \sqrt{\sum_{i=1}^{P} a_{ij}^2(\boldsymbol{x}^0) b_i} \cdot \left[(\phi(\gamma_j(\boldsymbol{x}^0)) - 1)\gamma_j(\boldsymbol{x}^0) + \frac{1}{\sqrt{2\pi}} e^{-\frac{1}{2}\gamma_j^2(\boldsymbol{x}^0)} \right]. \tag{32}$$

Following similar derivations, we can incorporate the PC coefficients into $\bar{u}_j(\boldsymbol{x}^0)$ for the lower specifications, $j \in \bar{J}_l$, as follows:

$$\bar{u}_j(\boldsymbol{x}^0) = \sqrt{\sum_{i=1}^{P} a_{ij}^2(\boldsymbol{x}^0) b_i} \cdot \left[\phi(\gamma_j(\boldsymbol{x}^0))\gamma_j(\boldsymbol{x}^0) + \frac{1}{\sqrt{2\pi}} e^{-\frac{1}{2}\gamma_j^2(\boldsymbol{x}^0)} \right]. \tag{33}$$

The proposed PC-based objective function $\bar{U}(\boldsymbol{x}^0)$ for yield-driven EM optimization including both upper and lower specifications is given as

$$\bar{U}(\boldsymbol{x}^0) = \sum_{j \in \bar{J}_u} \bar{u}_j(\boldsymbol{x}^0) + \sum_{j \in \bar{J}_l} \bar{u}_j(\boldsymbol{x}^0) \tag{34}$$

where $\bar{u}_j(\boldsymbol{x}^0)$ is given by (32) and (33) for upper ($j \in \bar{J}_u$) and lower specifications ($j \in \bar{J}_l$), respectively. By substituting (32) and (33) into (34), the proposed optimization objective function can be written in a more convenient form

$$\bar{U}(\boldsymbol{x}^0) = \sum_{j \in \bar{J}} V_j(\boldsymbol{x}^0) + \sum_{j \in \bar{J}_u} (a_{0j}(\boldsymbol{x}^0) - S_j) \tag{35}$$

where $V_j(\boldsymbol{x}^0)$ is computed from the PC coefficients as follows:

$$V_j(\boldsymbol{x}^0) = \sqrt{\sum_{i=1}^{P} a_{ij}^2(\boldsymbol{x}^0) b_i} \cdot \left[\phi(\gamma_j(\boldsymbol{x}^0))\gamma_j(\boldsymbol{x}^0) + \frac{1}{\sqrt{2\pi}} e^{-\frac{1}{2}\gamma_j^2(\boldsymbol{x}^0)} \right]. \tag{36}$$

Note that $a_{ij}(\boldsymbol{x}^0)$ are the PC coefficients, and $\gamma_j(\boldsymbol{x}^0)$ is computed from the PC coefficients $a_{ij}(\boldsymbol{x}^0)$ as shown in (30).

It is pointed out that through (20)–(36), we have changed the original objective function defined in (17) into a new form where the PC coefficients are incorporated. The PC coefficients are able to provide the statistical properties and approximate the PDF of the EM response with fewer EM samples than that required by the Monte Carlo analysis. Therefore, the new PC-based formulation requires fewer EM simulations to obtain accurate yield representation than the original formulation (which is based on assembling the responses evaluated at Monte Carlo samples). This advantage allows our proposed objective function to be able to facilitate the overall EM-based yield optimization process more efficiently.

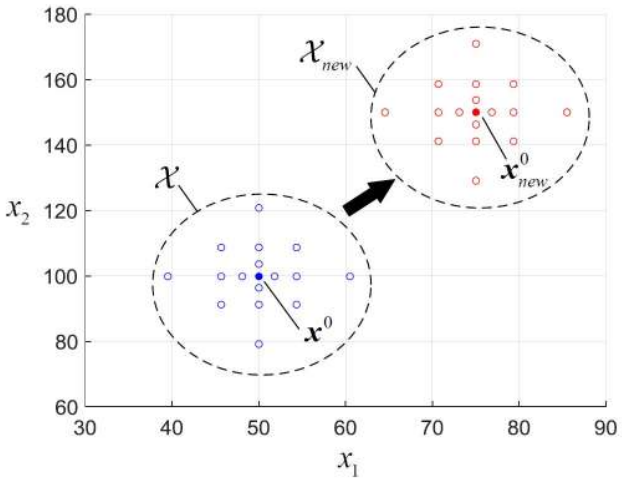

Fig. 1. Illustration of the movement of sparse grid samples in PC between two consecutive iterations during yield optimization. The two black dots represent the nominal points between two successive iterations. The circles represent the integration samples around the nominal points following the sparse grid technique. In yield optimization, the nominal point $\boldsymbol{x}^0$ is a variable which is updated iteratively. As the nominal point moves from $\boldsymbol{x}^0$ to $\boldsymbol{x}^0_{\text{new}}$, all the sparse grid samples move accordingly.

B. Derivation of Sensitivity Formulas for the Proposed Objective Function

To use the proposed objective function formulated earlier in yield-driven EM optimization, the derivatives of the proposed objective function $\bar{U}(\boldsymbol{x}^0)$ with respect to the varying nominal point $\boldsymbol{x}^0$ need to be derived so that a gradient-based optimization algorithm (e.g., quasi-Newton method) can be employed. In this section, we first derive the sensitivity formulas of PC coefficients with respect to $\boldsymbol{x}^0$, then derive the sensitivities for the objective function based on the sensitivity formulas of the PC coefficients.

At each iteration of the proposed yield optimization algorithm, a set of EM design parameters $\mathcal{X}$ is generated around the current nominal point $\boldsymbol{x}^0$ following the sparse grid technique, that is,

$$\mathcal{X} = \{T^{-1}(\boldsymbol{x}^0, \boldsymbol{\xi}^{(1)}), \ldots, T^{-1}(\boldsymbol{x}^0, \boldsymbol{\xi}^{(M)})\}. \tag{37}$$

Then, the PC coefficients are numerically evaluated using the EM responses simulated at these design parameters. The sparse grid samples are formed based on the Smolyak algorithm [41], which selectively combines the tensor products of lower order quadrature rules to cover the parameter space more efficiently [26]. As illustrated in Fig. 1, as the nominal point moves from $\boldsymbol{x}^0$ to $\boldsymbol{x}^0_{\text{new}}$, the sparse grid samples in the original parameter space move accordingly, forming a new set of sparse grid samples $\mathcal{X}_{\text{new}}$. In other words, the movement of the nominal point affects the location of every sparse grid

point in the original parameter space, which in turn affects each PC coefficient a_{ij}.

In this paper, we consider the design parameters to be Gaussian (normal) distributed and that the standard deviation is σ_d for the dth design parameter, $d = 1, 2, \ldots, n$. Then, the reverse transformation in (9) takes the following form:

$$T^{-1}(\boldsymbol{x}^0, \boldsymbol{\xi}^{(l)}) = \begin{bmatrix} x_1^0 \\ x_2^0 \\ \vdots \\ x_n^0 \end{bmatrix} + \begin{bmatrix} \sigma_1 \xi_1^{(l)} \\ \sigma_2 \xi_2^{(l)} \\ \vdots \\ \sigma_n \xi_n^{(l)} \end{bmatrix} \tag{38}$$

where $l = 1, \ldots, M$. Note that σ_d and $\xi_d^{(l)}$ are the predetermined constants for yield optimization.

Based on (11) and (38), we can obtain the derivatives of each PC coefficient $a_{ij}(\boldsymbol{x}^0)$ with respect to the nominal point $\boldsymbol{x}^0$ as follows:

$$\frac{\partial a_{ij}(\boldsymbol{x}^0)}{\partial \boldsymbol{x}^0} = \frac{1}{b_i} \sum_{l=1}^{M} \Phi_i(\boldsymbol{\xi}^{(l)}) w^{(l)} \frac{\partial R_j(\boldsymbol{x})}{\partial \boldsymbol{x}} \Big|_{\boldsymbol{x}=\boldsymbol{x}^{(l)}} \tag{39}$$

where $\boldsymbol{x}^{(l)} = T^{-1}(\boldsymbol{x}^0, \boldsymbol{\xi}^{(l)})$. $(\partial R_j(\boldsymbol{x})/\partial \boldsymbol{x}) \mid_{\boldsymbol{x}=\boldsymbol{x}^{(l)}}$ represents the EM sensitivities of $R_j(\boldsymbol{x})$ evaluated at the lth sparse grid point $\boldsymbol{x}^{(l)}$ in the original parameter space. These EM sensitivities can be obtained from the existing EM solvers with sensitivity analysis feature. b_i, $\Phi_i(\boldsymbol{\xi}^{(l)})$, and $w^{(l)}$ are the predetermined constants for yield optimization.

From (35) and (36), we can deduce the derivatives of the proposed objective function $\bar{U}(\boldsymbol{x}^0)$ with respect to each PC coefficient a_{ij} as follows:

$$\frac{\partial \bar{U}(\boldsymbol{x}^0)}{\partial a_{ij}} = \begin{cases} 1 - \phi(\gamma_j(\boldsymbol{x}^0)), & \text{for } i = 0,\ j \in \bar{J}_u \\ -\phi(\gamma_j(\boldsymbol{x}^0)), & \text{for } i = 0,\ j \in \bar{J}_l \\ 2a_{ij} b_i \dfrac{1}{\sqrt{2\pi}} \dfrac{1}{\sqrt{\sum_{p=1}^{P} a_{pj}^2(\boldsymbol{x}^0) b_p}} \cdot e^{-\frac{1}{2}\gamma_j^2(\boldsymbol{x}^0)}, & \text{for } i = 1, \ldots, P,\ j \in \bar{J}_u \cup \bar{J}_l. \end{cases} \tag{40}$$

The derivatives of the proposed objective function $\bar{U}(\boldsymbol{x}^0)$ with respect to the varying nominal point $\boldsymbol{x}^0$ can be found by

$$\frac{\partial \bar{U}(\boldsymbol{x}^0)}{\partial \boldsymbol{x}^0} = \sum_{i=0}^{P} \sum_{j \in \bar{J}} \frac{\partial \bar{U}(\boldsymbol{x}^0)}{\partial a_{ij}} \frac{\partial a_{ij}(\boldsymbol{x}^0)}{\partial \boldsymbol{x}^0} \tag{41}$$

where $(\partial \bar{U}(\boldsymbol{x}^0)/\partial a_{ij})$ and $(\partial a_{ij}(\boldsymbol{x}^0)/\partial \boldsymbol{x}^0)$ are given by (39) and (40), respectively.

C. PC-Based Yield Optimization Algorithm

In this section, we provide the detailed algorithm for the proposed PC-based yield-driven EM optimization.

First, a set of M samples $\{\boldsymbol{\xi}^{(1)}, \boldsymbol{\xi}^{(2)}, \ldots, \boldsymbol{\xi}^{(M)}\}$ is generated in the "$\boldsymbol{\xi}$-space" following the rules of the sparse grid technique. These samples are generated only once and would be reused in the subsequent iterations. The distribution pattern of the samples follows the rules of sparse grid techniques [36]. M is related to the accuracy level in sparse grid techniques. Increasing the accuracy level improves the multidimensional integration accuracy but results in a larger M, and thus requires more EM simulations. It is recommended that one fulfills the PC model construction at the initial nominal point before performing yield optimization for a specific EM structure to obtain the required minimal accuracy level. The minimal accuracy level can be obtained by starting from a small value and increasing it gradually until no significant integration difference can be observed between two successive accuracy levels.

Next, the M samples are transformed into EM geometrical parameter samples $\{T^{-1}(\boldsymbol{x}^0, \boldsymbol{\xi}^{(1)}),\ T^{-1}(\boldsymbol{x}^0, \boldsymbol{\xi}^{(2)}), \ldots, T^{-1}(\boldsymbol{x}^0, \boldsymbol{\xi}^{(M)})\}$ using (38). Then, an existing EM simulator is driven to evaluate the EM responses $R_j(T^{-1}(\boldsymbol{x}^0, \boldsymbol{\xi}^{(l)}))$ and the EM sensitivities $(\partial R_j(\boldsymbol{x})/\partial \boldsymbol{x}) \mid_{\boldsymbol{x}=\boldsymbol{x}^{(l)}}$, for $l = 1, 2, \ldots, M$. Since the responses and the sensitivities for different samples can be obtained independently, we evaluate the EM responses and the EM sensitivities at those M samples in parallel [42], [43]. By using this parallel computation scheme, we achieve additional speed up for EM-based yield optimization. Then, the PC coefficients $a_{ij}(\boldsymbol{x}^0)$ are numerically evaluated using (6)–(8) and the derivatives of each PC coefficient with respect to the nominal point are evaluated according to (39). Afterward, the proposed PC-based objective function $\bar{U}(\boldsymbol{x}^0)$ is evaluated using (35) and (36), while the derivatives $(\partial \bar{U}(\boldsymbol{x}^0)/\partial \boldsymbol{x}^0)$ are evaluated following (39)–(41).

Finally, $\bar{U}(\boldsymbol{x}^0)$ and $(\partial \bar{U}(\boldsymbol{x}^0)/\partial \boldsymbol{x}^0)$ are used in a gradient-based optimization algorithm (such as the quasi-Newton method) to find the update direction and suitable step size for the change of the nominal point from the current point $\boldsymbol{x}^0$ to a new point. Let the new nominal point be denoted as $\boldsymbol{x}_{\text{new}}^0$. The optimization terminates if the iteration counter N_{iter} exceeds the maximum iteration count $N_{\text{iter}}^{\max}$ or the difference of $\boldsymbol{x}^0$ between subsequent iterations is sufficiently small, that is,

$$N_{\text{iter}} > N_{\text{iter}}^{\max} \tag{42}$$

$$\text{or} \quad \left\| \boldsymbol{x}_{\text{new}}^0 - \boldsymbol{x}^0 \right\| < \varepsilon \tag{43}$$

where $N_{\text{iter}} = 0, 1, \ldots$. ε is a user-defined threshold. Fig. 2 shows the flowchart of the proposed PC-based yield optimization algorithm. The proposed algorithm can be summarized into the following steps.

- *Step 1:* Set the initial nominal point $\boldsymbol{x}_{\text{ini}}^0$ as the starting point for yield optimization, i.e., $\boldsymbol{x}^0 = \boldsymbol{x}_{\text{ini}}^0$. Typically, $\boldsymbol{x}_{\text{ini}}^0$ should be the optimal solution of nominal EM optimization. Initialize the iteration counter N_{iter} as 0. Set the maximum iteration number $N_{\text{iter}}^{\max}$ and the stopping criteria ε.
- *Step 2:* Generate M samples $\{\boldsymbol{\xi}^{(1)}, \boldsymbol{\xi}^{(2)}, \ldots, \boldsymbol{\xi}^{(M)}\}$ in the "$\boldsymbol{\xi}$-space" following the rules of the sparse grid technique.
- *Step 3:* Transform $\{\boldsymbol{\xi}^{(1)}, \boldsymbol{\xi}^{(2)}, \ldots, \boldsymbol{\xi}^{(M)}\}$ into a set of EM geometrical parameter samples around the nominal point using (38).
- *Step 4:* Evaluate the EM responses $R_j(T^{-1}(\boldsymbol{x}^0, \boldsymbol{\xi}^{(l)}))$ and the EM sensitivities $(\partial R_j(\boldsymbol{x})/\partial \boldsymbol{x}) \mid_{\boldsymbol{x}=\boldsymbol{x}^{(l)}}$, for $l = 1, 2, \ldots, M$, in parallel.

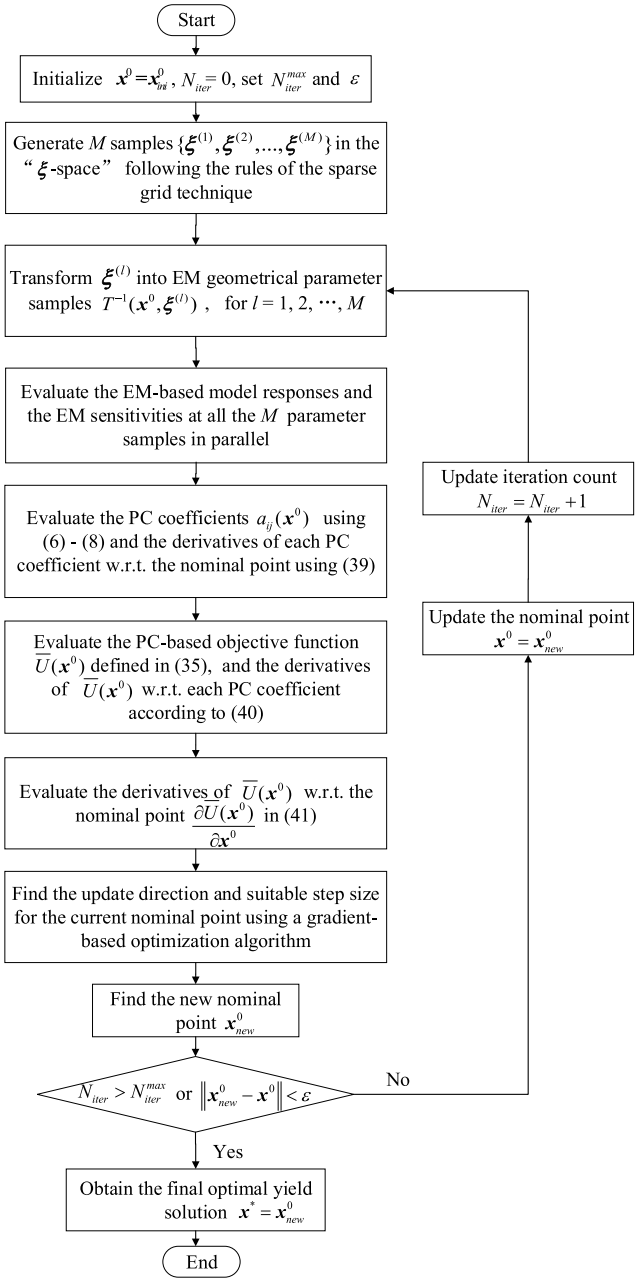

Fig. 2. Flowchart of the proposed PC-based yield optimization algorithm.

Step 5: Numerically evaluate the PC coefficients $a_{ij}(\boldsymbol{x}^0)$ using (6)–(8) and the derivatives of each PC coefficient with respect to the nominal point using (39).

Step 6: Evaluate the proposed PC-based objective function $\bar{U}(\boldsymbol{x}^0)$ defined in (35) and (36).

Step 7: Evaluate the derivatives of the proposed objective function $\bar{U}(\boldsymbol{x}^0)$ with respect to the nominal point $\boldsymbol{x}^0$ following (39)–(41).

Step 8: Find the update direction and suitable step size for the current nominal point using the gradient-based optimization algorithm (e.g., the quasi-Newton method), and find the new nominal point $\boldsymbol{x}^0_{\text{new}}$.

Step 9: If (42) or (43) is satisfied, go to step 10. Otherwise, update the nominal point $\boldsymbol{x}^0 = \boldsymbol{x}^0_{\text{new}}$, update the iteration count $N_{\text{iter}} = N_{\text{iter}} + 1$, and go to Step 3.

Step 10: Obtain the final optimal yield solution $\boldsymbol{x}^* = \boldsymbol{x}^0_{\text{new}}$. Stop the optimization process.

D. Discussion

In this paper, we have used normal distributions for the design parameters. In case other types of statistical distributions (e.g., uniform and log-normal) are needed, they can be accommodated by supplying different values of σ_d and $\xi_d^{(l)}$ in (38), and using different base functions $\Phi_i(\cdot)$ in (4). The values of σ_d are determined as the ratios between the sparse grid samples versus the corresponding samples in the physical/geometrical parameter space. Such ratios should be predetermined constants, which are fixed during yield optimization. The values of $\xi_d^{(l)}$ represent sparse grid samples. Different types of statistical distributions will have different sparse grid samples, and different base functions [35]. By supplying the proper values of σ_d and $\xi_d^{(l)}$ into (38), and proper base functions $\Phi_i(\cdot)$ into (4), our proposed approach can be applied to different types of statistical distributions.

Here, we provide a further discussion on the use of normal distributions for the design parameters in this paper. In theory, the value of random samples of normal distributions may have very large deviations since its domain is infinite. In our paper, this problem is avoided in developing the PC model by using sparse grid samples whose extreme values are defined to be limited within 1.73 times the standard deviation [26]. In generating testing samples for yield estimation, we limited the samples to be within three times the standard deviation. In this way, we retain the accuracy of the yield optimization method while avoiding values of random samples that are too large to be meaningful for EM simulation. If the required tolerance range is less than three times the standard deviation in normal distribution, then the distribution required will be truncated normal distribution. In this case, we need to treat it as a different distribution, i.e., we will require different values of σ_d and $\xi_d^{(l)}$ in (38) according to a different set of sparse grid samples, and supply different base functions $\Phi_i(\cdot)$ into (4) for the new distribution.

IV. Examples

A. Yield Optimization of a Waveguide K-Band Bandpass Filter

The first example under consideration is a waveguide K-band bandpass filter described in *ADS EMPro* tutorial document. The structure of the filter is shown in Fig. 3. The section of the waveguide where the filter is constructed is 10.668 mm × 4.318 mm (WR-42). The heights of three cylindrical posts are all 4.318 mm. r_1 is the radius of the two posts on the side while r_2 is the radius of the post in the middle. The two resonators placed between the cylindrical posts are of equal length d. The design parameters are $\boldsymbol{x} = [r_1\ r_2\ d]^T$ (mm). The design specifications are given by $|S_{11}| \leq -15$ dB, in the frequency range from 24.935 to 25.065 GHz, and $|S_{11}| \geq -1$ dB, in the frequency ranges from 24 to 24.75 GHz and from 25.25 to 26 GHz. The optimal nominal solution obtained by performing nominal EM optimization using *HFSS* is $\boldsymbol{x}^0_{\text{ini}} = [0.9597\ 1.7921\ 8.563]^T$ (mm).

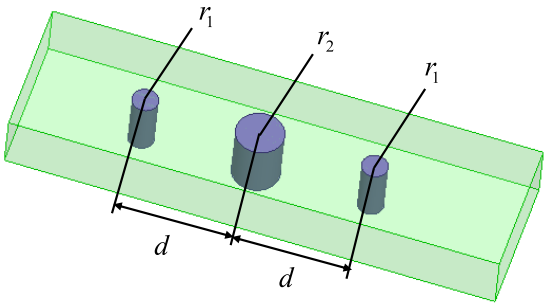

Fig. 3. Structure of the K-band bandpass filter example for EM simulation and yield optimization. The three design parameters of the filter are $\boldsymbol{x} = [r_1\ r_2\ d]^T$.

For yield analysis and optimization, we assume independent normal distribution for the design parameters, with the standard deviation being 5 μm. Both the Monte Carlo-based yield optimization approach presented in [1] and the proposed PC-based yield optimization approach are used to optimize the yield. For the proposed approach, Hermite polynomials are used and the PC expansion is truncated at total order $D = 2$. The 1-D Kronrod–Patterson [36] quadrature rule is used to form a 3-D total-order grid. An integration accuracy level 3 is required for this example, which results in the total number of quadrature points M being 19. To find the reasonable value of N for the Monte Carlo-based yield optimization approach, we run a Monte Carlo analysis to estimate the yield at the initial nominal point. By varying the number of random samples, a convergence on the yield value is observed when $N = 50$. For comparison purpose, we use $N = 19$, $N = 30$, and $N = 50$ for the Monte Carlo-based yield optimization approach.

Quasi-Newton method is used as the gradient-based optimization algorithm to find the optimal yield solution iteratively for both approaches. At each iteration of optimization, HFSS is driven to evaluate the EM responses and the EM sensitivities at all the parameter samples in parallel. To find the optimal yield solutions, we set the maximum number of iterations to be a large number to allow both optimization approaches to converge. When the optimization process terminates, we verify the yield at the optimal yield solution by running a Monte Carlo analysis with 100 random samples for the two approaches.

For this example, we also perform yield optimization using a third approach, i.e., the *ADS* internal yield optimization tool with *EMPro*. A parametrized 3-D structure of the K-band bandbass filter is created using *EMPro*. Then, the nominal EM optimization is performed in *ADS* to find an optimal nominal solution. Two nominal solutions that can meet the design specifications are found, i.e., $\boldsymbol{x}^0_{\text{ini}} = [1.2069\ 2.1315\ 9.1955]^T$ (mm) (case 1) and $\boldsymbol{x}^0_{\text{ini}} = [1.1785\ 2.0811\ 9.1094]^T$ (mm) (case 2). Following this, yield estimation is conducted using the yield estimation tool in *ADS* for both cases. Finally, we take these two nominal solutions as starting points and use the built-in yield optimization tool in *ADS* to optimize the yield. We stop the yield optimization process until no significant yield increase can be observed.

TABLE I
COMPARISON OF YIELD OPTIMIZATION RESULTS FOR THE K-BAND BANDPASS FILTER

Yield optimization approach	# of EM simulations per iteration	Initial yield	Final yield	Total # of EM simulations
Monte Carlo-based	19	41%	52%	247
	30	41%	56%	1050
	50	41%	59%	1700
Proposed	19	41%	60%	532
ADS yield optimization (case 1)	N/A	33%	49%	3350
ADS yield optimization (case 2)	N/A	35%	47%	3180

Table I summarizes the yield optimization results of three yield optimization approaches for this example. As can be seen from the table, all the three approaches achieve improvements of the yield. However, the total number of EM simulations required by the Monte Carlo-based yield optimization approach and the proposed approach are much fewer than that required by the built-in yield optimizer in *ADS*. The reason for this is that the Monte Carlo-based yield optimization approach and the proposed approach use sensitivity information and gradient-based optimization algorithms in the yield optimization process. From Table I, it can also be observed that to achieve a similar yield increase, the proposed PC-based approach requires much fewer EM simulations than the Monte Carlo-based yield optimization approach. This is because by incorporating the PC coefficients into the formulation of the yield optimization objective function, the proposed approach requires fewer EM simulations to find the effective direction and suitable step size for the update of the nominal point at each iteration of optimization than the Monte Carlo-based yield optimization approach. Fig. 4 shows the yield before and after optimization using the proposed approach for the K-band bandpass filter. The optimal yield solution found by the proposed approach is $[0.9643\ 1.7779\ 8.554]^T$ (mm).

To further demonstrate the advantages of the proposed approach, we perform another numerical experiment by deliberately stopping the Monte Carlo-based yield optimizations at certain iteration such that the total number of EM simulations during optimization is similar to that in the proposed approach. Table II gives the comparison of yield improvements under this consideration. It can be seen from the table that using similar number of EM simulations, the proposed approach achieves a greater yield improvement than the Monte Carlo-based yield optimization approach. The reason for this is that the proposed PC-based approach provides more effective direction and step size for the update of the nominal point than that the Monte Carlo-based yield optimization approach provides. As a result, with similar number of EM simulations, the proposed approach is able to provide more promising yield increase than the Monte Carlo-based yield optimization approach.

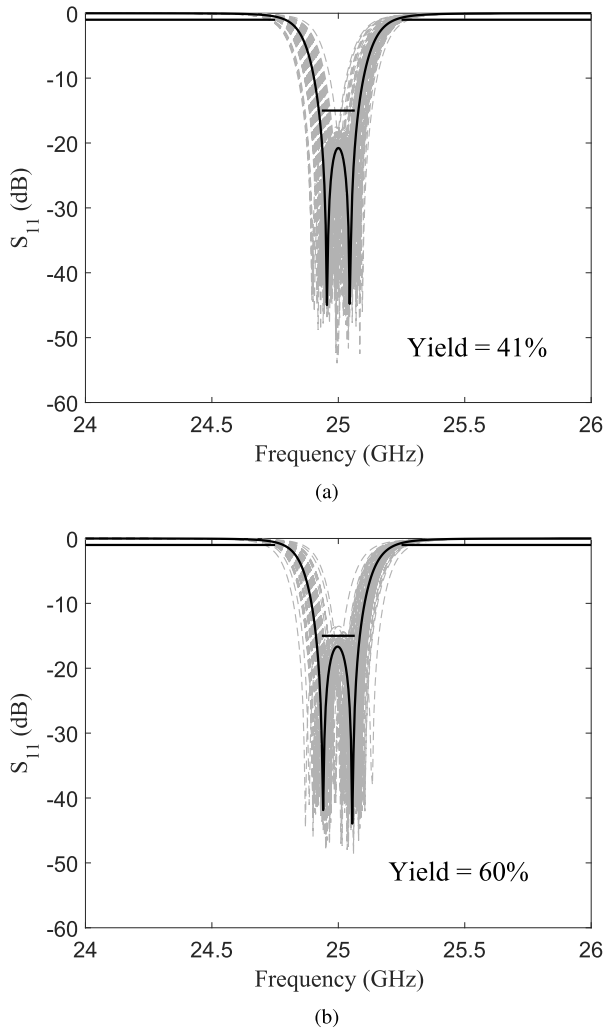

Fig. 4. Yield optimization results of the K-band bandpass filter. (a) Before yield optimization. (b) After yield optimization. Gray dashed lines: 100 samples from Monte Carlo analysis. Black solid line: response evaluated at the nominal point.

TABLE II

COMPARISON OF YIELD IMPROVEMENTS WITH SIMILAR NUMBER OF EM SIMULATIONS FOR THE K-BAND BANDPASS FILTER

Yield optimization approach	# of EM simulations per iteration	Initial yield	Final yield	Total # of EM simulations
Monte	30	41%	53%	540
Carlo-based	50	41%	55%	550
Proposed	19	41%	60%	532

B. Yield Optimization of a Waveguide Bandpass Filter With Fractal-Shaped Irises

In the second example, we consider a waveguide bandpass filter with fractal-shaped irises (FSIs), as shown in Fig. 5 [44]. The design parameters are $\boldsymbol{x} = [d_1\ d_2\ d_3]^T$ (mm), where d_1, d_2, and d_3 represent the distances between the first, second, and third pair of symmetrical irises, respectively. An example of the geometrical dimensions of the FSIs is given in Fig. 6. The section of the waveguide is $a = 22.86$ mm and

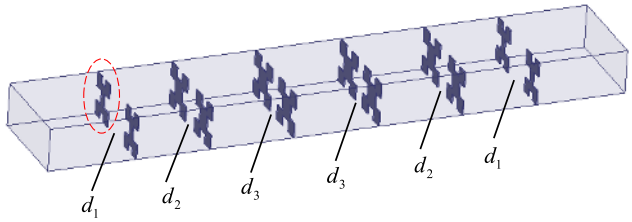

Fig. 5. Structure of the waveguide bandpass filter example with FSIs for EM simulation and yield optimization. The three design parameters of the filter are $\boldsymbol{x} = [d_1\ d_2\ d_3]^T$.

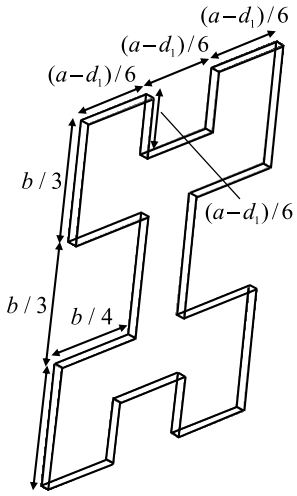

Fig. 6. Details of the geometrical structure of the FSI as circled in Fig. 5.

$b = 10.16$ mm (WR-90). The design specification for this filter is given by $|S_{11}| \leq -22$ dB, in the frequency range from 9.2 to 9.8 GHz. The optimal nominal solution $\boldsymbol{x}_{\text{ini}}^0 = [9.3444\ 4.9203\ 3.7423]^T$ (mm) is obtained by performing nominal EM optimization [45].

We assume independent normal distributions for all design parameters to allow yield estimation and optimization. The standard deviation for each design parameter is assumed to be 20 μm. The proposed approach and the Monte Carlo-based yield optimization approach are both used to optimize the yield. For the proposed approach, Hermite polynomials are used and the integration accuracy level required is three for the sparse grid technique. This results in the number of sparse grid samples $M = 19$. For the Monte Carlo-based yield optimization approach, it is found that $N = 100$ is suitable to represent the statistics of all the possible outcomes. For comparison purpose, different number of random samples ($N = 19, 50, 100$) per iteration are used for the Monte Carlo-based yield optimization approach. The maximum iteration count is set to be a large number to allow both optimization approaches to converge.

Table III gives a comparison between the two approaches in terms of the final yield and the total number of EM simulations required during optimization. From the table, we can conclude that the proposed method achieves the greatest yield increase among four cases of optimizations compared. It can also be

TABLE III

COMPARISON OF YIELD OPTIMIZATION RESULTS FOR THE WAVEGUIDE FSI FILTER

Yield optimization approach	# of EM simulations per iteration	Initial yield	Final yield	Total # of EM simulations
Monte Carlo-based	19	67%	69%	304
	50	67%	72%	900
	100	67%	79%	1100
Proposed	19	67%	84%	475

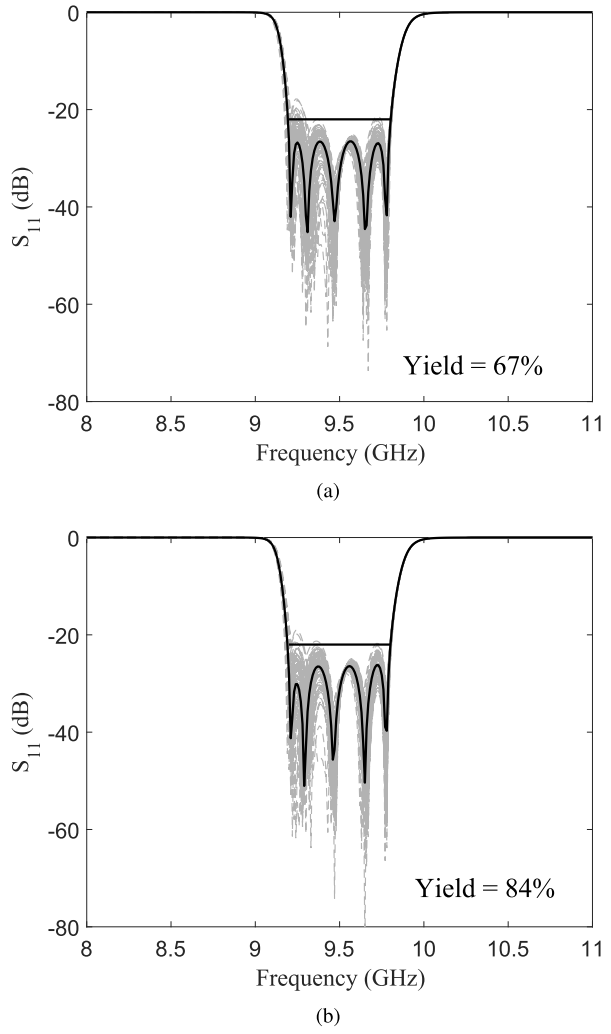

Fig. 7. Yield optimization results of the waveguide bandpass filter with FSIs. (a) Before yield optimization. (b) After yield optimization. Gray dashed lines:100 samples from Monte Carlo analysis. Black solid line: response evaluated at the nominal point.

observed that to achieve a similar yield increase, the total number of EM simulations required by the proposed approach is less than half of that required by the Monte Carlo-based yield optimization approach. This reduction allows us to achieve a substantial speed up for the overall EM-based yield optimization process. Fig. 7 shows the yield of the waveguide FSI filter before and after optimization using the proposed approach. The optimal yield solution found by the proposed approach is $[9.3682\ 4.9542\ 3.7585]^T$ (mm).

TABLE IV

COMPARISON OF YIELD IMPROVEMENTS WITH SIMILAR NUMBER OF EM SIMULATIONS FOR THE WAVEGUIDE FSI FILTER

Yield optimization approach	# of EM simulations per iteration	Initial yield	Final yield	Total # of EM simulations
Monte Carlo-based	50	67%	70%	450
	100	67%	75%	500
Proposed	19	67%	84%	475

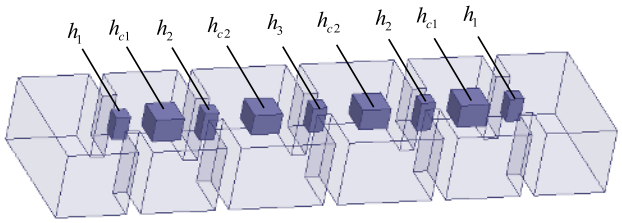

Fig. 8. Structure of the four-pole waveguide filter example for EM simulation and yield optimization, with design parameters $\boldsymbol{x} = [h_1\ h_2\ h_3\ h_{c1}\ h_{c2}]^T$.

To further demonstrate the advantages of the proposed approach, we perform another numerical experiment by deliberately stopping the Monte Carlo-based yield optimizations at a certain iteration so that the total number of EM simulations used is similar to that in the proposed approach. The yield improvements achieved by the two approaches under this condition are given in Table IV. It can be seen from the table that using similar number of EM simulations, the proposed approach achieves a greater yield improvement than the Monte Carlo-based yield optimization approach. The reason is that the proposed PC-based objective function provides more accurate yield representation, and thus, more effective direction and step size for updating the nominal point than the conventional Monte Carlo-based yield optimization approach.

C. Yield Optimization of a Four-Pole Waveguide Filter

Finally, the proposed approach is applied to yield optimization of a four-pole waveguide filter [45]. The structure of the waveguide filter is shown in Fig. 8, with five design parameters $\boldsymbol{x} = [h_1\ h_2\ h_3\ h_{c1}\ h_{c2}]^T$ (mm). h_1, h_2, and h_3 represent the heights of posts in the coupling windows, while h_{c1} and h_{c2} are the heights of posts in the resonant cavities. The thickness of all the coupling windows is set to be 2 mm. The design specification is given by $|S_{11}| \leq -16$ dB, in the frequency range from 10.85 to 11.15 GHz. The optimal nominal solution $\boldsymbol{x}^0_{\text{ini}} = [3.407\ 4.083\ 3.571\ 3.295\ 2.978]^T$ (mm) is obtained by performing nominal EM optimization [45].

The design parameters are assumed to be independently normal distributed around their nominal values with 10-μm standard deviation. Before performing yield optimization, the Monte Carlo analysis is used to estimate the yield at the optimal nominal solution. By varying the number of random samples from 51 to 300, we observe a convergence on the yield value (53%) when $N = 300$. For this example, Hermite polynomials are used and the accuracy level required is three

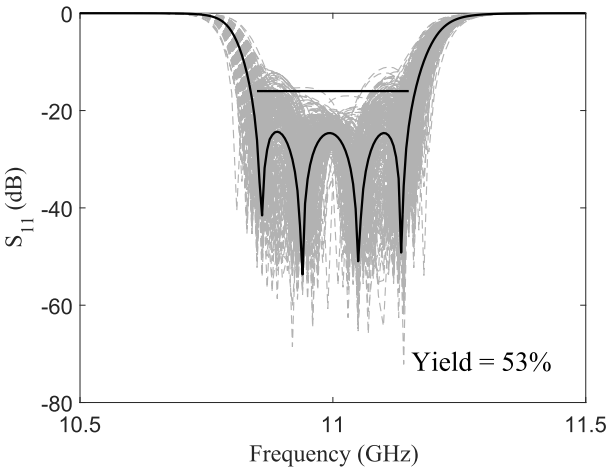

(a)

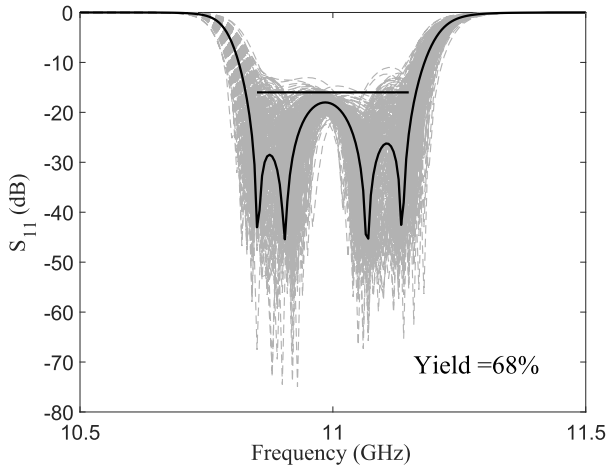

(b)

Fig. 9. Yield optimization results of the four-pole waveguide filter. (a) Before yield optimization. (b) After yield optimization. Gray dashed lines: 300 samples from Monte Carlo analysis. Black solid line: response evaluated at the nominal point.

for the sparse grid technique. This results in the number of sparse grid samples $M = 51$.

Yield optimization is then performed using the proposed approach with $M = 51$. For comparison purpose, we also use the Monte Carlo-based yield optimization approach with $N = 51, 75, 100, 200$ to optimize the yield. The final yield is verified by performing a Monte Carlo analysis with 300 random samples at the optimal yield solution. Fig. 9 shows the initial yield and the yield after optimization using the proposed approach for this example. The optimal yield solution found by the proposed approach is $[3.3913\ 4.1464\ 3.6241\ 3.3019\ 2.9776]^T$ (mm). The yield optimization results are summarized in Tables V and VI. It can be observed from Table V that the proposed approach achieves the greatest yield increase among the five cases of optimizations compared. To achieve a similar yield increase, the proposed approach requires much fewer EM simulations than the Monte Carlo-based yield optimization approach. A substantial speed up for the overall yield optimization process has been achieved. As a further comparison given in Table VI, it can be observed that using similar number of EM simulations, the proposed approach achieves a greater yield improvement than the Monte Carlo-based yield optimization approach.

TABLE V
COMPARISON OF YIELD OPTIMIZATION RESULTS FOR THE FOUR-POLE WAVEGUIDE FILTER

Yield optimization approach	# of EM simulations per iteration	Initial yield	Final yield	Total # of EM simulations
Monte Carlo-based	51	53%	58%	1173
	75	53%	62%	1575
	100	53%	63%	2800
	200	53%	67%	4400
Proposed	51	53%	68%	1275

TABLE VI
COMPARISON OF YIELD IMPROVEMENTS WITH SIMILAR NUMBER OF EM SIMULATIONS FOR THE FOUR-POLE WAVEGUIDE FILTER

Yield optimization approach	# of EM simulations per iteration	Initial yield	Final yield	Total # of EM simulations
Monte Carlo-based	75	53%	58%	1275
	100	53%	60%	1300
	200	53%	64%	1400
Proposed	51	53%	68%	1275

V. CONCLUSION

We have proposed a novel PC-based approach to yield-driven EM optimization. The computational advantages of the PC approach have been exploited to facilitate EM-based yield optimization of microwave structures. The PC coefficients have been incorporated into the formulation of the optimization objective function such that the number of EM simulations required to obtain effective update direction and suitable step size of the nominal point is reduced. Sensitivity formulas have been derived for both the PC coefficients and the proposed objective function with respect to the yield optimization variables. Compared with the conventional Monte Carlo-based yield optimization approach, the proposed approach is able to achieve similar yield increase using much fewer EM simulations or greater yield increase with similar number of EM simulations. The proposed approach helps to achieve high-quality solutions in shorter time for the challenging problem of yield-driven EM optimization. As a possible future direction, the proposed method can be applied to increase the yield in the manufacturing process of a real microwave component.

REFERENCES

[1] J. W. Bandler and S. H. Chen, "Circuit optimization: The state of the art," *IEEE Trans. Microw. Theory Techn.*, vol. 36, no. 2, pp. 424–443, Feb. 1988.

[2] R. Biernacki, S. Chen, G. Estep, J. Rousset, and J. Sifri, "Statistical analysis and yield optimization in practical RF and microwave designs," in *IEEE MTT-S Int. Microw. Symp. Dig.*, Montreal, QC, Canada, Jun. 2012, pp. 1–3.

[3] D. E. Hocevar, M. R. Lightner, and T. N. Trick, "An extrapolated yield approximation technique for use in yield maximization," *IEEE Trans. Comput.-Aided Design Integr. Circuits Syst.*, vol. CAD-3, no. 4, pp. 279–287, Oct. 1984.

[4] A. H. Zaabab, Q.-J. Zhang, and M. Nakhla, "A neural network modeling approach to circuit optimization and statistical design," *IEEE Trans. Microw. Theory Techn.*, vol. 43, no. 6, pp. 1349–1358, Jun. 1995.

[5] K. Singhal and J. Pinel, "Statistical design centering and tolerancing using parametric sampling," *IEEE Trans. Circuits Syst.*, vol. CAS-28, no. 7, pp. 692–702, Jul. 1981.

[6] H. L. Abdel-Malek, A.-K. S. O. Hassan, and M. H. Heaba, "Statistical circuit design with the use of a modified ellipsoidal technique," *Int. J. Microw. Millim.-Wave Comput.-Aided Eng.*, vol. 7, no. 1, pp. 117–129, Jan. 1997.

[7] H. L. Abdel-Malek and J. W. Bandler, "Yield estimation for efficient design centring assuming arbitrary statistical distributions," *Int. J. Circuit Theory Appl.*, vol. 6, no. 3, pp. 289–303, 1978.

[8] H. L. Abdel-Malek, A.-K. S. O. Hassan, and M. H. Heaba, "A boundary gradient search technique and its applications in design centering," *IEEE Trans. Comput.-Aided Design Integr. Circuits Syst.*, vol. 18, no. 11, pp. 1654–1660, Nov. 1999.

[9] J. W. Bandler, R. M. Biernacki, S. H. Chen, P. A. Grobelny, and R. H. Hemmers, "Space mapping technique for electromagnetic optimization," *IEEE Trans. Microw. Theory Techn.*, vol. 42, no. 12, pp. 2536–2544, Dec. 1994.

[10] J. E. Rayas-Sanchez, "EM-based optimization of microwave circuits using artificial neural networks: The state-of-the-art," *IEEE Trans. Microw. Theory Techn.*, vol. 52, no. 1, pp. 420–435, Jan. 2004.

[11] M. A. Ismail, D. Smith, A. Panariello, Y. Wang, and M. Yu, "EM-based design of large-scale dielectric-resonator filters and multiplexers by space mapping," *IEEE Trans. Microw. Theory Techn.*, vol. 52, no. 1, pp. 386–392, Jan. 2004.

[12] J. V. M. Ros *et al.*, "Fast automated design of waveguide filters using aggressive space mapping with a new segmentation strategy and a hybrid optimization algorithm," *IEEE Trans. Microw. Theory Techn.*, vol. 53, no. 4, pp. 1130–1142, Apr. 2005.

[13] N. K. Nikolova, X. Zhu, Y. Song, A. Hasib, and M. H. Bakr, "*S*-parameter sensitivities for electromagnetic optimization based on volume field solutions," *IEEE Trans. Microw. Theory Techn.*, vol. 57, no. 6, pp. 1526–1538, Jun. 2009.

[14] F. Feng, C. Zhang, V.-M.-R. Gongal-Reddy, Q.-J. Zhang, and J. Ma, "Parallel space-mapping approach to EM optimization," *IEEE Trans. Microw. Theory Techn.*, vol. 62, no. 5, pp. 1135–1148, May 2014.

[15] J. W. Bandler, J. E. Rayas-Sánchez, and Q.-J. Zhang, "Yield-driven electromagnetic optimization via space mapping-based neuromodels," *Int. J. RF Microw. Comput.-Aided Eng.*, vol. 12, no. 1, pp. 79–89, 2002.

[16] H. L. Abdel-Malek, A. S. O. Hassan, E. A. Soliman, and S. A. Dakroury, "The ellipsoidal technique for design centering of microwave circuits exploiting space-mapping interpolating surrogates," *IEEE Trans. Microw. Theory Techn.*, vol. 54, no. 10, pp. 3731–3738, Oct. 2006.

[17] Q. S. Cheng, J. W. Bandler, and S. Koziel, "Response corrected tuning space mapping for yield estimation and design centering," in *IEEE MTT-S Int. Microw. Symp. Dig.*, Anaheim, CA, USA, May 2010, p. 1.

[18] A.-K. S. O. Hassan, A. S. A. Mohamed, and A. Y. El-Sharabasy, "Statistical microwave circuit optimization via a non-derivative trust region approach and space mapping surrogates," in *IEEE MTT-S Int. Microw. Symp. Dig.*, Baltimore, MD, USA, Jun. 2011, pp. 1–4.

[19] J. W. Bandler, R. M. Biernacki, S. H. Chen, P. A. Grobelny, and R. H. Hemmers, "Exploitation of coarse grid for electromagnetic optimization," in *IEEE MTT-S Int. Microw. Symp. Dig.*, San Diego, CA, USA, May 1994, pp. 381–384.

[20] S. Koziel and A. Bekasiewicz, "Low-cost surrogate-assisted statistical analysis of miniaturized microstrip couplers," *J. Electromagn. Waves Appl.*, vol. 30, no. 10, pp. 1345–1353, 2016.

[21] S. Koziel and J. W. Bandler, "Rapid yield estimation and optimization of microwave structures exploiting feature-based statistical analysis," *IEEE Trans. Microw. Theory Techn.*, vol. 63, no. 1, pp. 107–114, Jan. 2015.

[22] C. Zhang, W. Na, Q. J. Zhang, and J. W. Bandler, "Fast yield estimation and optimization of microwave filters using a cognition-driven formulation of space mapping," in *IEEE MTT-S Int. Microw. Symp. Dig.*, San Francisco, CA, USA, May 2016, pp. 1–4.

[23] D. Xiu and G. E. Karniadakis, "The Wiener–askey polynomial chaos for stochastic differential equations," *SIAM J. Sci. Comput.*, vol. 24, no. 2, pp. 619–644, 2002.

[24] A. C. M. Austin and C. D. Sarris, "Efficient analysis of geometrical uncertainty in the FDTD method using polynomial chaos with application to microwave circuits," *IEEE Trans. Microw. Theory Techn.*, vol. 61, no. 12, pp. 4293–4301, Dec. 2013.

[25] T.-A. Pham, E. Gad, M. S. Nakhla, and R. Achar, "Decoupled polynomial chaos and its applications to statistical analysis of high-speed interconnects," *IEEE Trans. Compon., Packag., Manuf. Technol.*, vol. 4, no. 10, pp. 1634–1647, Oct. 2014.

[26] A. C. M. Austin, N. Sood, J. Siu, and C. D. Sarris, "Application of polynomial chaos to quantify uncertainty in deterministic channel models," *IEEE Trans. Antennas Propag.*, vol. 61, no. 11, pp. 5754–5761, Nov. 2013.

[27] P. Sumant, H. Wu, A. Cangellaris, and N. Aluru, "Reduced-order models of finite element approximations of electromagnetic devices exhibiting statistical variability," *IEEE Trans. Antennas Propag.*, vol. 60, no. 1, pp. 301–309, Jan. 2012.

[28] D. V. Ginste, D. De Zutter, D. Deschrijver, T. Dhaene, P. Manfredi, and F. G. Canavero, "Stochastic modeling-based variability analysis of on-chip interconnects," *IEEE Trans. Compon., Packag., Manuf. Technol.*, vol. 2, no. 7, pp. 1182–1192, Jul. 2012.

[29] P. Manfredi, D. Vande Ginste, D. De Zutter, and F. G. Canavero, "Improved polynomial chaos discretization schemes to integrate interconnects into design environments," *IEEE Microw. Wireless Compon. Lett.*, vol. 23, no. 3, pp. 116–118, Mar. 2013.

[30] A. K. Prasad, M. Ahadi, and S. Roy, "Multidimensional uncertainty quantification of microwave/RF networks using linear regression and optimal design of experiments," *IEEE Trans. Microw. Theory Techn.*, vol. 64, no. 8, pp. 2433–2446, Aug. 2016.

[31] M. Ahadi and S. Roy, "Sparse linear regression (SPLINER) approach for efficient multidimensional uncertainty quantification of high-speed circuits," *IEEE Trans. Comput.-Aided Design Integr. Circuits Syst.*, vol. 35, no. 10, pp. 1640–1652, Oct. 2016.

[32] P. Manfredi, D. Vande Ginste, D. De Zutter, and F. G. Canavero, "Uncertainty assessment of lossy and dispersive lines in SPICE-type environments," *IEEE Trans. Compon., Packag., Manuf. Technol.*, vol. 3, no. 7, pp. 1252–1258, Jul. 2013.

[33] M. R. Rufuie, E. Gad, M. Nakhla, and R. Achar, "Generalized Hermite polynomial chaos for variability analysis of macromodels embedded in nonlinear circuits," *IEEE Trans. Compon., Packag., Manuf. Technol.*, vol. 4, no. 4, pp. 673–684, Apr. 2014.

[34] A. K. Prasad and S. Roy, "Accurate reduced dimensional polynomial chaos for efficient uncertainty quantification of microwave/RF networks," *IEEE Trans. Microw. Theory Techn.*, vol. 65, no. 10, pp. 3697–3708, Oct. 2017.

[35] M. S. Eldred, "Recent advances in non-intrusive polynomial chaos and stochastic collocation methods for uncertainty analysis and design," in *Proc. 50th AIAA/ASME/ASCE/AHS/ASC Struct., Struct. Dyn., Mater. Conf.*, Palm Springs, CA, USA, May 2009, pp. 1–37.

[36] F. Heiss and V. Winschel, "Likelihood approximation by numerical integration on sparse grids," *J. Econ.*, vol. 144, no. 1, pp. 62–80, 2008.

[37] X. Li, J. Le, P. Gopalakrishnan, and L. T. Pileggi, "Asymptotic probability extraction for non-normal distributions of circuit performance," in *Proc. IEEE/ACM Int. Conf. Comput. Aided Design*, Nov. 2004, pp. 2–9.

[38] Z. Zhang, N. Farnoosh, T. Klemas, and L. Daniel, "Maximum-entropy density estimation for MRI stochasitc surrogate models," *IEEE Antennas Wireless Propag. Lett.*, vol. 13, pp. 1656–1659, Aug. 2014.

[39] N. M. Steen, G. D. Byrne, and E. M. Gelbard, "Gauss quadratures for the integrals $\int_0^\infty exp(-x^2)f(x)dx$ and $\int_0^b exp(-x^2)f(x)dx$," *Math. Comput.*, vol. 23, no. 107, pp. 661–671, 1969.

[40] A. Papoulis, *Probability—Random Variables and Stochastic Processes*. New York, NY, USA: McGraw-Hill, 1991.

[41] D. Xiu, "Efficient collocational approach for parametric uncertainty analysis," *Commun. Comput. Phys.*, vol. 2, no. 2, pp. 293–309, 2007.

[42] J. Zhang, K. Ma, F. Feng, and Q. Zhang, "Parallel gradient-based local search accelerating particle swarm optimization for training microwave neural network models," in *IEEE MTT-S Int. Microw. Symp. Dig.*, Phoenix, AZ, USA, May 2015, pp. 1–3.

[43] J. Zhang, K. Ma, F. Feng, Z. Zhao, W. Zhang, and Q. Zhang, "Distributed parallel computing technique for EM modeling," in *Proc. IEEE MTT-S Int. Conf. Numer. Electromagn. Multiphys. Modeling Optim. (NEMO)*, Ottawa, ON, Canada, Aug. 2015, pp. 1–3.

[44] D. Oloumi, A. Kordzadeh, and A. A. Lotfi Neyestanak, "Size reduction and bandwidth enhancement of a waveguide bandpass filter using fractal-shaped irises," *IEEE Antennas Wireless Propag. Lett.*, vol. 8, pp. 1214–1217, Oct. 2009.

[45] C. Zhang, F. Feng, V.-M.-R. Gongal-Reddy, Q. J. Zhang, and J. W. Bandler, "Cognition-driven formulation of space mapping for equal-ripple optimization of microwave filters," *IEEE Trans. Microw. Theory Techn.*, vol. 63, no. 7, pp. 2154–2165, Jul. 2015.

Jianan Zhang (S'15) was born in Tieling, Liaoning, China, in 1991. He received the B.Eng. degree from Tianjin University, Tianjin, China, in 2013. He is currently pursuing the Ph.D. degree at the School of Microelectronics, Tianjin University, Tianjin, China, and the Cotutelle Ph.D. degree at the Department of Electronics, Carleton University, Ottawa, ON, Canada.

His current research interests include statistical modeling, electromagnetic (EM)-based yield optimization of microwave structures, uncertainty quantification using polynomial chaos, computational electromagnetics, and space mapping-based EM optimization.

Chao Zhang (S'14) was born in Xinyang, Henan, China, in 1990. He received the B.Eng. and M.Eng. degrees from Tianjin University, Tianjin, China, in 2012 and 2014, respectively. He is currently pursuing the Ph.D. degree at the Department of Electronics, Carleton University, Ottawa, ON, Canada.

In 2010, he was an Exchange Student with the National Taipei University of Technology, Taipei, Taiwan. His current research interests include design, modeling, and optimization of microwave circuits, and space mapping techniques.

Mr. Zhang was a recipient of the National Scholarship for Graduate Students in China in 2013 and the Indira Gandhi Fellowship in Carleton University in 2016.

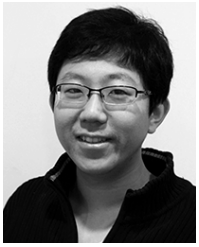

Feng Feng (S'13–M'17) was born in Huludao, China, in 1990. He received the B.Eng. degree from Tianjin University, Tianjin, China, in 2012, and the Ph.D. degree from the School of Microelectronics, Tianjin University, Tianjin, China, and from the Department of Electronics, Carleton University, Ottawa, ON, Canada, in 2017.

He is currently a Post-Doctoral Fellow with the Department of Electronics, Carleton University. His current research interests include microwave circuit design and modeling, optimization theory and algorithms, space mapping and surrogate model optimization, and electromagnetic field simulation and optimization.

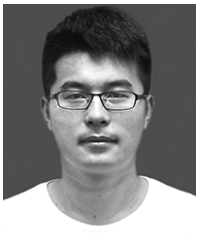

Wei Zhang (S'15) was born in Qingdao, Shandong, China, in 1989. He received the B.Eng. degree from Shandong University, Jinan, Shandong, China, in 2013. He is currently pursuing the Ph.D. degree at the School of Microelectronics, Tianjin University, Tianjin, China, and the Cotutelle Ph.D. degree at the Department of Electronics, Carleton University, Ottawa, ON, Canada.

His current research interests include microwave device modeling, space mapping and surrogate modeling, and multiphysics simulation and optimization.

Jianguo Ma (M'96–SM'97–F'16) received the B.Sc. and M.Sc. degrees from Lanzhou University, Lanzhou, China, in 1982 and 1988, respectively, and the Ph.D. degree in engineering from Duisburg University, Duisburg, Germany, in 1996.

From 1996 to 1997, he was a Post-Doctoral Fellow with the Technical University of Nova Scotia, Halifax, NS, Canada. From 1997 to 2005, he was a faculty member with Nanyang Technological University, Singapore, where he was also the Founding Director of the Center for Integrated Circuits and Systems. From 2005 to 2009, he was with the University of Electronic Science and Technology of China, Chengdu, China. Since 2008, he has been the Technical Director of the Tianjin IC Design Center. From 2009 to 2016, he was the Dean of the School of Electronic Information Engineering, Tianjin University, Tianjin, China. He is currently with the School of Computer Science and Technology, Guangdong University of Technology, Guangzhou, China. He has authored or co-authored about 245 technical papers and 2 books. He holds 6 U.S. patents and 15 filed/granted China patents. His current research interests include RFICs and RF integrated systems for wireless, RF device characterization modeling, monolithic microwave integrated circuit, RF/microwave circuits and systems, and electromagnetic interference in wireless, RFID, and wireless sensing networks.

Dr. Ma is currently a member of the Editorial Board for the PROCEEDINGS OF THE IEEE. He was a recipient of the Prestigious Changjiang (Yangtze) Scholar Award of the Ministry of Education of China in 2007 and the Distinguished Young Investigator Award of the National Natural Science Foundation of China in 2006. He served as an Associate Editor for IEEE MICROWAVE AND COMPONENTS LETTERS from 2004 to 2005.

Qi-Jun Zhang (S'84–M'87–SM'95–F'06) received the B.Eng. degree from the Nanjing University of Science and Technology, Nanjing, China, in 1982, and the Ph.D. degree in electrical engineering from McMaster University, Hamilton, ON, Canada, in 1987.

From 1982 to 1983, he was with the System Engineering Institute, Tianjin University, Tianjin, China. From 1988 to 1990, he was with Optimization Systems Associates Inc., Dundas, ON, Canada, where he developed advanced microwave optimization software. In 1990, he joined the Department of Electronics, Carleton University, Ottawa, ON, Canada, where he is currently a Full Professor. He is also an Adjunct Professor with the School of Microelectronics, Tianjin University. He has authored or co-authored over 260 publications, authored *Neural Networks for RF and Microwave Design* (Artech House, 2000), coedited *Modeling and Simulation of High-Speed VLSI Interconnects* (Kluwer, 1994), and contributed to the *Encyclopedia of RF and Microwave Engineering* (Wiley, 2005), *Fundamentals of Nonlinear Behavioral Modeling for RF and Microwave Design* (Artech House, 2005), and *Analog Methods for Computer-Aided Analysis and Diagnosis* (Marcel Dekker, 1988). His current research interests include microwave CAD and neural network and optimization methods for high-speed/high-frequency circuit design.

Dr. Zhang is a Fellow of the Electromagnetics Academy and the Canadian Academy of Engineering. He is a member of the Editorial Board of the IEEE TRANSACTIONS ON MICROWAVE THEORY AND TECHNIQUES. He is a Co-Chair of the Technical Committee on CAD (MTT-1) of the IEEE Microwave Theory and Techniques Society. He was a Guest Co-Editor for the "Special Issue on High-Speed VLSI Interconnects" for the *International Journal of Analog Integrated Circuits and Signal Processing* (Kluwer, 1994), and twice was a Guest Editor for the "Special Issue on Applications of ANN to RF and Microwave Design" for the *International Journal of RF and Microwave Computer-Aided Engineering* (Wiley, 1999 and 2002). He is an Associate Editor for the *International Journal of RF and Microwave Computer-Aided Engineering*.